Petroleum Science 20 (2023) 3110–3118

Contents lists available at ScienceDirect

Petroleum Science

journal homepage: www.keaipublishing.com/en/journals/petroleum-science

Original Paper

Synthesis and mechanism of environmentally friendly high temperature and high salt resistant lubricants

Zong-Lun Wang [a], Jin-Sheng Sun [a, b, **], Jing-Ping Liu [a, *], Kai-He Lv [a], Zi-Hua Shao [a], Xian-Fa Zhang [a], Zhe Xu [a], Zhi-Wen Dai [a], Ning Huang [a]

[a] School of Petroleum Engineering, China University of Petroleum (East China), Qingdao 266580, Shandong, China
[b] CNPC Engineering Technology R & D Company Limited, Beijing 102206, China

ARTICLE INFO

Article history:
Received 6 October 2022
Received in revised form
19 January 2023
Accepted 9 May 2023
Available online 16 May 2023

Edited by Jia-Jia Fei

Keywords:
Deep oil and gas
Lubricant
Environmentally friendly
Water-based drilling fluid
Molecular dynamics simulations

ABSTRACT

With the exploration and development of deep and ultra-deep oil and gas, high torque and high friction during the drilling of deep and ultra-deep wells become one of the key issues affecting drilling safety and drilling speed. Meanwhile, the high temperature and high salt problem in deep formations is prominent, which poses a major challenge to the lubricity of drilling fluids under high temperature and high salt. This paper reports an organic borate ester SOP as an environmentally friendly drilling fluid lubricant. The performance evaluation results show that when 1% lubricant SOP is added to the fresh water-based mud, the lubrication coefficient decreases from 0.631 to 0.046, and the reduction rate of lubrication coefficient is 92.7%. Under the conditions of 210 °C and 30% NaCl, the reduction rate of lubricating coefficient of the base slurry with 1% SOP was still remain 81.5%. After adding 1% SOP, the wear volume decreased by 94.11% compared with the base slurry. The contact resistance experiment during the friction process shows that SOP can form a thick adsorption film on the friction surface under high temperature and high salt conditions, thus effectively reducing the friction resistance. Molecular dynamics simulation shows that lubricant SOP can be physically adsorbed on the surface of drilling tool and borehole wall through hydrogen bond and van der Waals force. XPS analysis further shows that SOP adsorbs on the friction surface and reacts with metal atoms on the friction surface to form a chemically reactive film. Therefore, under high temperature and high salt conditions, the synergistic effect of physical adsorption film and chemical reaction film effectively reduces the frictional resistance and wear of the friction surface. In addition, SOP is non-toxic and easy to degrade. Therefore, SOP is a highly effective and environmentally friendly lubricant in high temperature and high salt drilling fluid.

1. Introduction

With the exploration and development of deep and ultra deep oil and gas, the high torque and high friction in the drilling process of deep and ultra deep wells have become one of the key problems affecting the drilling safety and penetration rate (Aarrestad, 1994; Sönmez et al., 2013; Dong et al., 2015; Liu et al., 2021). As the blood of drilling engineering, drilling fluid plays an important role in lubrication during the drilling process (David et al., 2017). Oil-based drilling fluids and synthetic-based drilling fluids have a better lubrication effect than water-based drilling fluids (Razali et al., 2018; Humood et al., 2019; Lan et al., 2020). However, the high cost and pollution problems of oil-based and synthetic-based drilling fluids have limited their development. The development of high-performance water-based drilling fluids has not only greatly reduced the performance gap with oil-based drilling fluids, but also achieved low cost and environmental protection (Li et al., 2015).

One of the most common methods to reduce torque and drag in water-based drilling fluids is to add lubricants to the water-based drilling fluid (Briscoe et al., 2001; Ma et al., 2009; Tadros, 2011; Nomura et al., 2012; Livescu and Craig, 2017). Drilling fluid lubricants can be divided into two categories: solid lubricants and liquid

* Corresponding author.
** Corresponding author. School of Petroleum Engineering, China University of Petroleum (East China), Qingdao 266580, Shandong, China.
E-mail addresses: sunjsdri@cnpc.com.cn (J.-S. Sun), liujingping20@126.com (J.-P. Liu).

https://doi.org/10.1016/j.petsci.2023.05.005

lubricants (Chhowalla and Amaratunga, 2000; McGuiggan et al., 2007). Solid lubricants include graphite and glass balls, but they tend to affect solid phase control in the drilling process. And they are usually difficult to degrade (Teer, 2001; Shaji and Radhakrishnan, 2003; Xiao et al., 2016; Liu et al., 2017). Liquid lubricants can be divided into mineral oil, poly alpha-olefin, fatty acid ester, and polymeric alcohols categories according to their main components (Zhou et al., 2013; Kania et al., 2015; Xiao et al., 2017; Paswan and Mahto, 2020; Saidi et al., 2020). Among them, mineral oil lubricants have better temperature and salt resistance, but they are more toxic, have poor biodegradability and high fluorescence level; other liquid lubricants have poor lubrication holding properties, low extreme pressure film strength, poor temperature resistance and great impact on the environment, which are difficult to meet the drilling engineering needs of deep wells, directional wells, large slope, and large displacement wells in oil and gas fields (Borugadda and Goud, 2016). Therefore, there is an urgent need to develop a high-performance environmental protection drilling fluid lubricant that is suitable for high abrasion resistance torque, high temperature, and high salt environment.

Organoboric acid esters can be considered as derivatives of boric acid in which hydrogen is replaced by organic groups. As an effective extreme pressure anti-wear agent with non-toxic, good lubricity and excellent friction reduction, and anti-wear properties, organoborate ester is an important grease additive and has been widely used in lubricant oil, which can improve the extreme pressure anti-wear ability of lubricant oil. Philipbon et al. investigated a borate ester as a lubricant oil additive and showed that the borate ester can form borate ions by friction and thus react with iron oxide on the rigid surface to form a borate-iron network (Philippon et al., 2011). Zheng et al. investigated the use of borate esters containing nitrogen atoms as additives to lubricant oil, and showed that borate esters have better friction reduction and anti-wear properties than the conventional lubricant additive zinc dialkyl dithiophosphate (ZnDTP) (Zheng et al., 1998). However, as far as I know, there are few reports on the use of organoboric acid esters as drilling fluid lubricants. Only borate nanoparticles have been studied as water-based drilling fluid lubricants. Saffari et al. found that borate nanoparticles can roll on the friction surface and thus change the nature of wear from pure sliding friction to mixed rolling-sliding friction to improve the lubricity and extreme pressure performance of water-based drilling fluids (Saffari et al., 2018). But borate nanoparticles may not have good lubricating properties under high temperature and high salt conditions (Shah et al., 2013; Saffari et al., 2018). Herein, in this paper, a temperature resistant, salt resistant and environment-friendly organic borate ester environmental lubricant SOP for drilling fluid was synthesized by using boric acid as raw material and reacting with long-chain fatty acids and polyols, and its structure and lubrication properties were discussed and analyzed. More importantly, the adsorption capacity and kinetic behavior were investigated using molecular dynamics simulations. The mechanism of action of SOP was analyzed by contact resistance experiments and XPS tests. The environmental friendliness of the lubricant SOPs was also tested.

2. Experimental section

2.1. Materials

D-sorbitol (AR), phosphoric acid (AR), boric acid (AR), oleic acid (AR) and sodium hydroxide (AR) was purchased from Aladdin Chemical Reagent Co. Glycerol monooleate (GM) is from Jiangsu Haian Petrochemical Co. HEP-1 is an anti-temperature and anti-salt lubricant made from mineral oil, compounded with extreme pressure additives containing sulfur and nitrogen, purchased from Shandong Deshunyuan Co. Bentonite used for preparing base slurry is provided by Huai'an Bentonite Company. 20 g of bentonite and 0.8 g of Na_2CO_3 were added to 400 mL of water, stirred at 6000 r/min for 30 min, and sealed airtight at room temperature for 24 h to obtain a water-based drilling fluid base slurry (Chang et al., 2019b; Sun et al., 2020).

2.2. Synthesis of the SOP lubricant

Add 18.2 g sorbitol and 0.09 g phosphoric acid into a four neck flask equipped with a condensing tube and a stirrer, and react at 160 °C for 90 min under nitrogen. After adding 6.2 g boric acid, the reaction time was 3 h. Then 28.2 g oleic acid and 0.15 g sodium hydroxide were added. The temperature was increased to 200 °C and react for 4 h. After cooling, amber viscous liquid is obtained, which is lubricant SOP. Fig. 1 shows the SOP preparation process.

2.3. Characterizations of the SOP

Fourier transform infrared spectroscopy FTIR (IR Tracer-100 Shimadzu Corporation) revealed the structure of the highly efficient extreme pressure lubricant SOP, where the scanning wavelength was 400–4000 cm^{-1}. The thermal properties of SOP in the temperature range of 40–800 °C were analyzed by a thermogravimetric analyzer (Mettler Toledo Co. Switzerland) at a nitrogen purge and a heating rate of 10 °C/min.

2.4. Lubrication coefficient test

The lubrication coefficient test is used to characterize the frictional resistance between the drilling column and the well wall or casing under the rotation of the drilling column (Sönmez et al., 2013). The lubrication coefficient μ in the drilling fluid was measured with an EP-B type extreme pressure lubricator (Model: EP-B, Shande Petroleum Instrument Company, CHINA). The extreme pressure (EP) test is performed by applying the measured normal force to a torque-sensitive rotating bearing cup using a torque arm. During the dynamic friction test, a torque of 150 inch-pounds was applied to the steel block and the block was pressed against a steel ring rotating at 60 rpm, and the friction coefficient reading was recorded after 5 min. If all ring block metallurgy is the same, the lubrication coefficient values for water are 34 at 60 rmp and 150 inch-pounds. However, since they are not the same values, a correction factor is used. The lubrication factor is calculated according to Eq. (1). To further describe the lubrication effect, the percentage reduction in the lubrication coefficient was used to quantify the lubrication performance, as shown in Eq. (2).

$$\mu = \frac{N_1 \times 34}{100 \times N_2} \tag{1}$$

where μ is the lubrication coefficient, N_1 is the friction reading in the specimen, N_2 is the friction reading in deionized water, 34 is the correction factor.

$$R = \frac{(\mu_B - \mu_S)}{\mu_B} \times 100\% \tag{2}$$

where R is the reduction rate of lubrication coefficient, μ_B is the lubrication coefficient in 5% base slurry, and μ_S is the lubrication reading in 5% base slurry with added lubricant.

From Eq. (1), it can be found that the lower the lubrication coefficient, the lower the friction between the drilling column and the well wall or casing. All results were performed at room temperature.

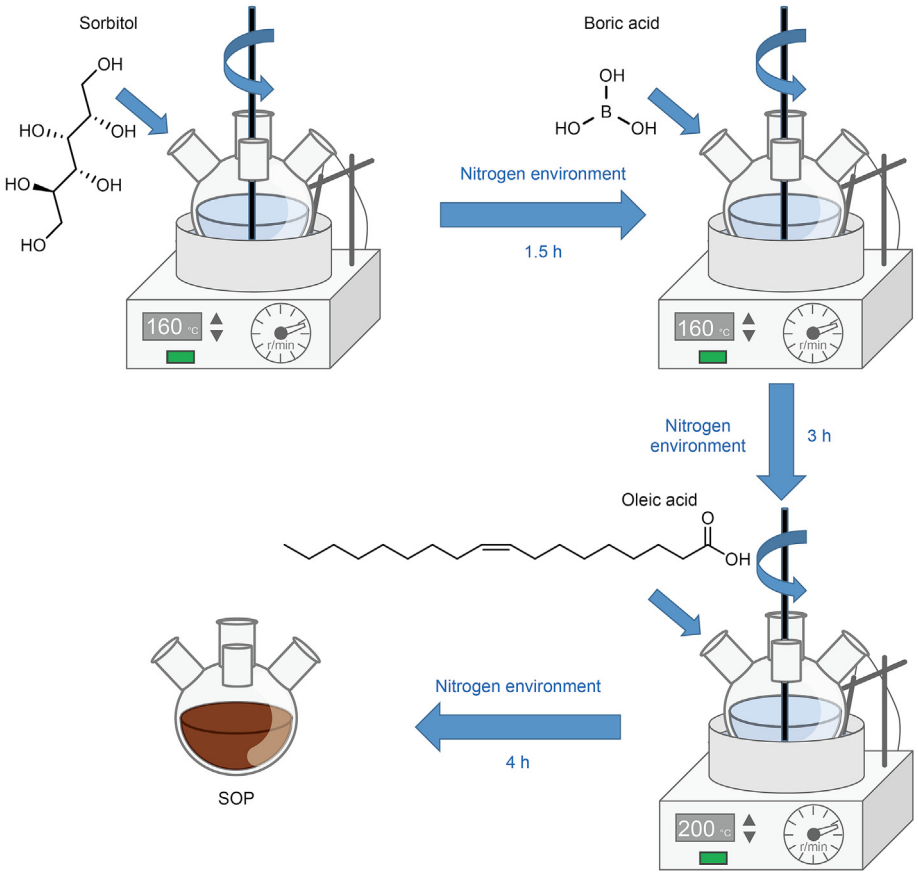

Fig. 1. Schematic diagram of preparation processes for SOP.

2.5. Tribological test

The real-time friction coefficient (COF) and wear loss (WV) of the lubricant on the steel surface were tested by a friction and wear tester. The micro vibration friction and wear tester SRV-IV is used for vibration and reciprocating motion. The friction test method has load = 100 N, frequency = 25 Hz, and amplitude = 1 mm. Tribological tests were conducted on base pastes containing 30% NaCl and different types of lubricants after aging at 210 °C for 16 h.

2.6. Contact resistance test of friction surface

The contact resistance during real-time friction is obtained by connecting the resistance wires in the friction and wear tester SRV-IV.

2.7. X-ray photoelectron spectroscopy (XPS) tests

The elemental distribution photoelectron spectroscopy of the friction film formed on the sliding rough surface in the tribological test was tested by X-ray photoelectron spectroscopy (Nexa, Thermo Fisher Inc.).

2.8. Models and simulations

Molecular dynamics (MD) simulations are set up to investigate the interaction of the SOP lubricant with drilling tools and wellbore, respectively. All simulations were conducted in the Forcite module using Materials Studio. The model consisted of three layers, the size of which was 4.030 nm × 4.030 nm × 7.343 nm. The lattice parameters and atomic position information of ferric oxide unit cell were obtained from diffraction experiments, and the atomic position information of silicon oxide were obtained from the American Mineralogist Crystal Structure Database. 8 × 8 × 1 unit cell ferric oxide was the upper and bottom layer in the model. The SOP lubricant solution was placed between two layers of ferric oxide or silicon oxide to investigate the direct contact of lubricant molecules and the oxide layer on the steel surface or wellbore (Berro et al., 2010). The solution phase contained 8 SOP molecules and 2000 water molecules randomly distributed at a concentration of 9.5%. COMPASS force field cannot deal with the system containing the boron element and therefore the full periodic table force field (UFF) is selected instead. Universal force field (UFF) (Rappe et al., 1992) was employed to depict the interaction of water molecules, organics, and metal oxide atoms (Bahlakeh et al., 2018; Ramezanzadeh et al., 2019). After geometry optimization by conjugate gradient method, the simulations were carried out for 1 ns with the NVT ensembles. The time step was 1 fs. The outer layer of ferric oxide or silicon oxide is fixed during geometry optimization and the NVT simulation. The temperature was set at 393.15 K controlled by the Andersen thermostat to simulate the general bottom wellbore condition.

2.9. Environmental aspects

In recent years, billions of tons of toxic oilfield waste have

flowed into the sea due to improper treatment, causing serious harm to plants, animals, and the environment. Therefore, environmental friendliness is crucial to the current development of oilfield treatment agents. The biological toxicity of SOP was determined according to GB/T 18420.2-2009 standard. The percentage of light loss (EC_{50}) indicates the biological toxicity of the test sample. The biodegradability test was determined according to GB/T 11914-2017 and HJ 505-2009 standards. The ratio of BOD_5 and COD indicates the biodegradability of the samples (Aarrestad, 1994; Ji et al., 2002; Pi et al., 2015; Chang et al., 2019a; Sun et al., 2022).

3. Results and discussion

3.1. Characterization of the SOP lubricant

Fig. 2 shows the infrared spectrum of SOP of the synthetic product. The peaks corresponding to 3397 and 3211 cm^{-1} from the IR spectrum were identified as stretching vibration peaks of −OH. The characteristic peaks of 2923 and 2857 cm^{-1} are stretching vibrational peaks of $-CH_2-$. The characteristic peak near 1736 cm^{-1} was identified as the telescopic vibrational peak of −COO−. The peak at 1622 cm^{-1} corresponds to the telescopic vibrational peak of −C=C− on oleic acid. And 1161 cm^{-1} is the telescopic vibrational peak of −B−O−C− peak. The infrared spectra proved that the target products were successfully prepared.

As shown in Fig. 3, the mass loss process of SOP is divided into three parts. The first part occurs in the temperature range from 40 to 340 °C (mass loss of about 16.21%), and the mass loss in this phase is mainly the evaporation of intra- and intermolecular water, which is due to the absorption of free water from the air by a large number of hydrophilic groups in the SOP. When the temperature rises, the volatilization of free water leads to a partial mass loss of SOP. In the second part, the thermogravimetric (TGA) curve decreases sharply in the temperature range from 340 to 422 °C, and the mass loss of SOP is 75.54%. The mass loss of SOP at this stage mainly corresponds to the thermal decomposition of functional groups in the SOP molecule and the breakage of the main chain, resulting in partial mass loss of the product. The third part of the mass loss of SOP is after 422 °C, when the molecular chain of SOP is completely broken and the whole molecule is completely decomposed. Usually, the thermal degradation of SOP mainly occurs above 340 °C, which indicates that SOP has good thermal stability.

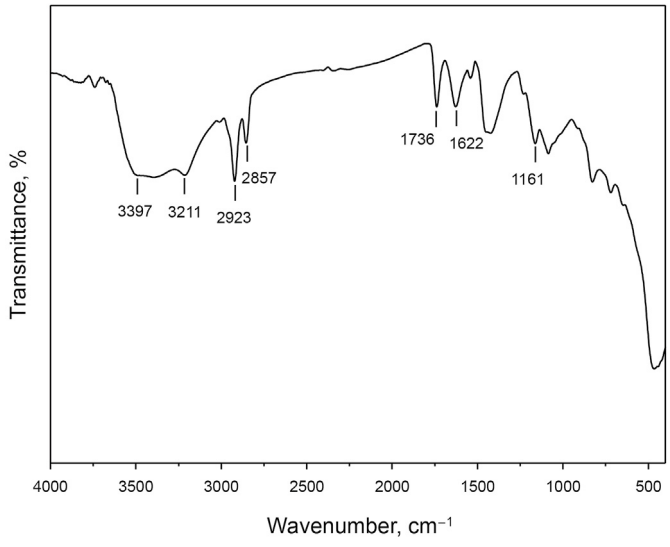

Fig. 2. FTIR spectrum of SOP.

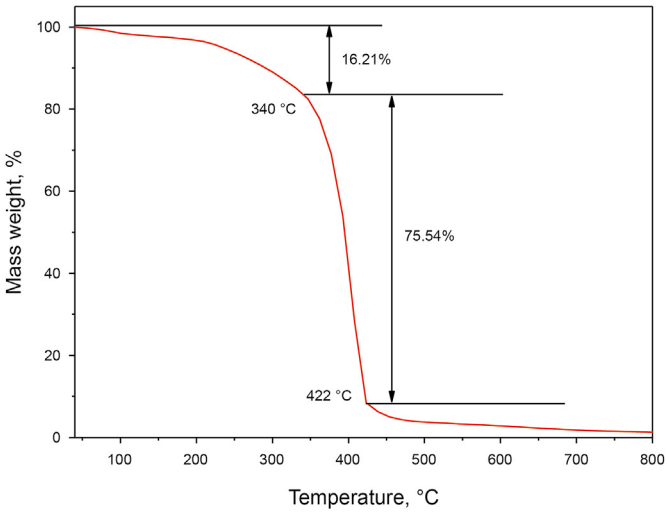

Fig. 3. Mass loss curves of SOP relative to increasing temperature.

3.2. Lubrication behavior

3.2.1. Lubrication coefficient test

The lubrication coefficient test is one of the most common tests to evaluate the frictional resistance between the drilling column and the well wall or casing as it rotates. The lubrication coefficient test results are shown in Fig. 4. Fig. 4(a) shows that the lubrication coefficient of 5.0% base slurry is as high as 0.631. When 1% SOP is added to the base slurry, the lubrication coefficient is reduced to 0.046. And the reduction rate of lubrication coefficient is as high as 92.7%, which shows good lubrication performance. And the lubrication coefficient decreases with the increase of lubricant SOP concentration. Fig. 4(b) shows the change curve of lubrication coefficient of base slurry with 1% SOP added relative to different concentrations of sodium chloride before hot rolling (BHR) and after hot rolling (AHR) at 210 °C for 16 h. With the increase of NaCl concentration, the lubrication coefficient of the base slurry before and after aging increased, but the overall remained at a low level. When the NaCl concentration increased to 35%, the lubrication coefficient after aging was 0.118. The reduction of lubrication coefficient was kept at 79.4%, which showed excellent salt resistance performance. Fig. 4(c) shows the lubrication coefficient of the base slurry with different lubricants added before and after aging at 210 °C for 16 h. The lubrication coefficient of 5% base slurry was 0.647 after aging at 210 °C. After adding 1% GM and 1% HEP-1, the lubrication coefficients decreased to 0.122 and 0.107, respectively, which were both higher than that of the lubricant SOP at 0.062. This indicates that the lubrication effect of SOP was better than that of the currently used lubricant. As shown in Fig. 4(d), the lubrication coefficient of the base slurry with 30% NaCl added is 0.573 after aging at 210 °C. The lubrication coefficient drops to 0.256 and 0.196 after adding 1% GM and 1% HEP-1, respectively, while the lubrication coefficient drops to 0.106 after adding 1% SOP. And the reduction rate of lubrication coefficient of 1% SOP is as high as 81.5%, which indicates that SOP can still show excellent lubrication performance under high temperature and high salt conditions. In addition, its temperature and salt resistance is better than the commonly used lubricants GM and HEP-1.

3.2.2. Tribological test

Fig. 5(a) shows the COF of different samples in the friction and wear experiments. The COF is significantly lower with the addition of lubricant. Compared with GM and HEP-1, SOP has stronger lubrication and anti-wear properties in high temperature and high

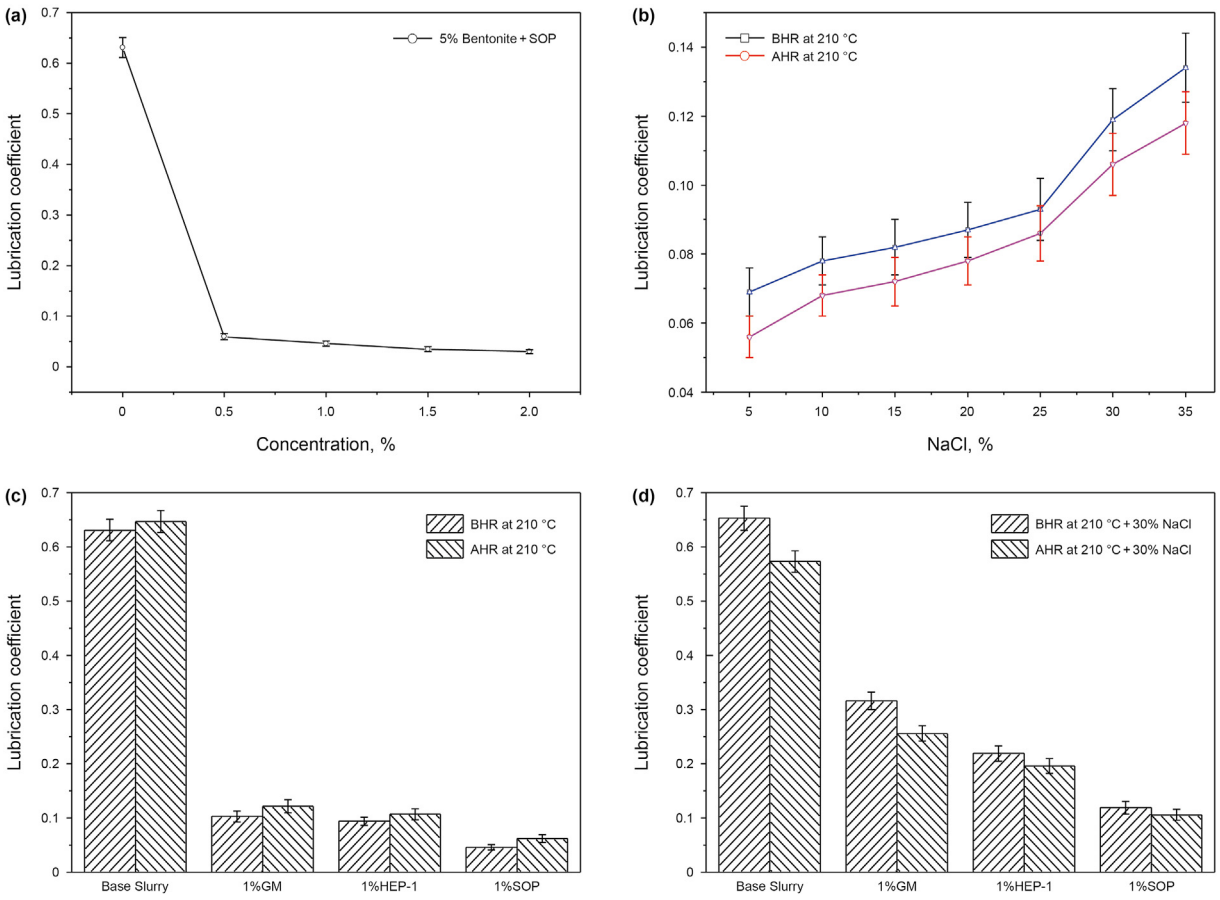

Fig. 4. Lubrication coefficient of base slurry at different concentrations of SOP (**a**). The change curve of lubrication coefficient of base slurry with 1% SOP added relative to different concentrations of sodium chloride before hot rolling (BHR) and after hot rolling (AHR) at 210 °C for 16 h (**b**). Lubrication coefficient of base slurry with different lubricants before and after hot rolling at 210 °C for 16 h (**c**). Lubrication coefficient of base slurry with different lubricants added at 30% NaCl before and after hot rolling at 210 °C for 16 h (**d**).

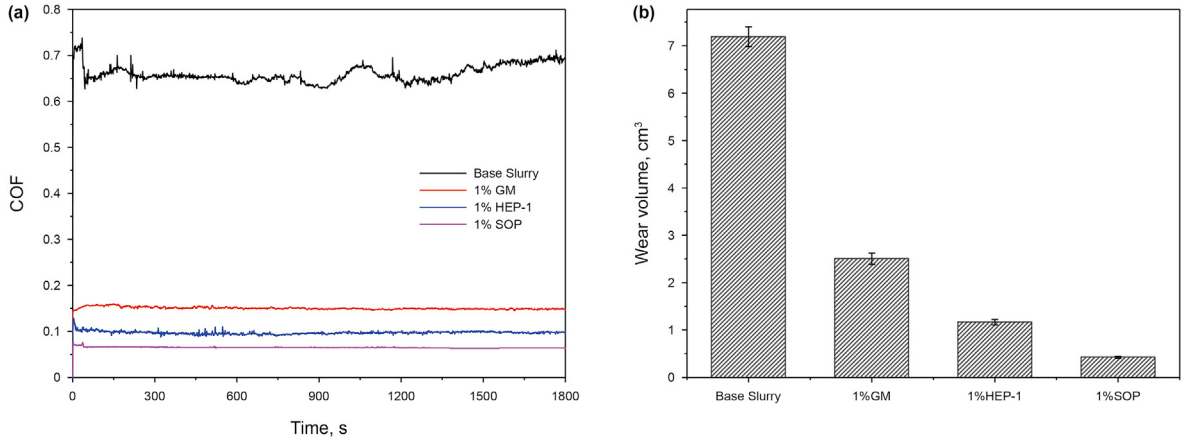

Fig. 5. COFs of different lubricants (**a**) and WV values of worn surfaces lubricated by different lubricants (**b**).

salt conditions, which is consistent with the results in the lubrication coefficient experiment. As shown in Fig. 5(b), the wear volume experiments showed that SOP could effectively enhance the wear resistance of drilling fluid and reduce the wear of drilling tools. This is more clearly demonstrated by the 3D morphology diagram of the wear surface (Fig. 6). This is mainly due to the targeted adsorption of polar groups in SOP and the shear resistance of flexible long alkyl chains.

3.3. Contact resistance analysis

Contact resistance (R) refers to the resistance formed in the actual contact area which allows timely monitoring the formation of the friction film formation process of the lubricant on the friction surface. Fig. 7 shows the average contact resistance of surfaces lubricated by different lubricants. The R-value in the base slurry is close to zero, which indicates that the base slurry cannot form an

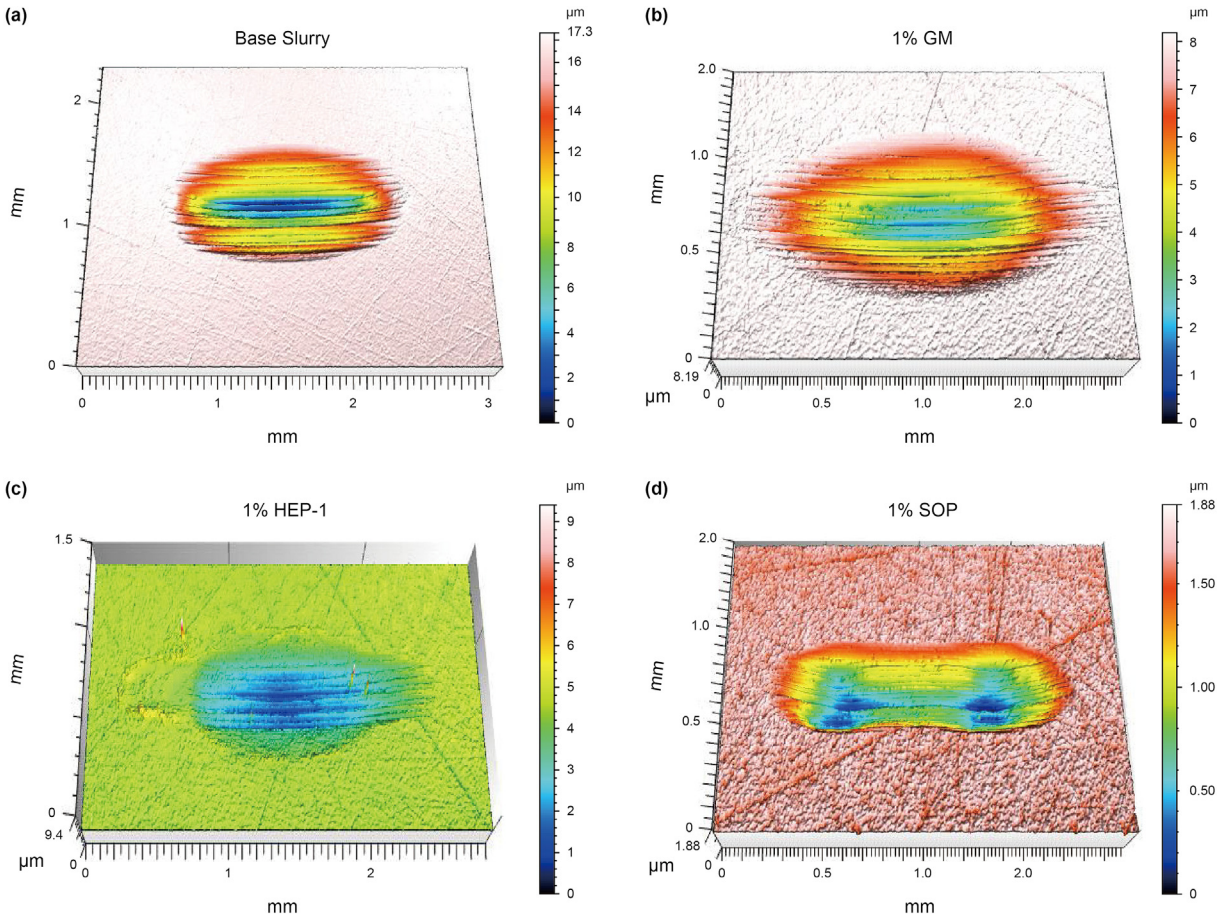

Fig. 6. 3D morphology of worn surfaces lubricated by different lubricants.

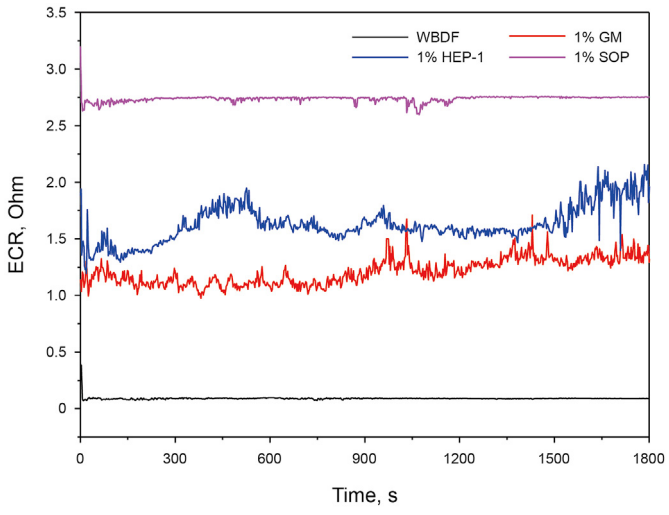

Fig. 7. Average electrical contact resistance measurement for surfaces lubricated by different lubricants.

effective surface film at the friction surface. This may result in direct contact between the steel plates. The *R*-value increases significantly with the addition of lubricant, which is due to the lubricant's ability to create a strong adsorption film at the contact surface, thus effectively impeding the friction between the steel plates. For SOP, the highest *R*-value means that SOP forms a thicker adsorption film on the friction surface even under high temperature and high salt conditions, resulting better lubrication performance, which is consistent with the results of friction wear experiments and lubrication coefficient experiments (Dong et al., 2020).

3.4. Molecular dynamics simulations

MD simulations were conducted to observe the adsorption process of SOP molecules on the surface of drilling tools to verify the proposed mechanism. As shown in Fig. 8, the polar head groups of SOP molecules were absorbed on the ferric oxide surface. Ester groups and hydroxyl groups were in direct contact with the metal surface, and the alkyl chains pointed to the interior of the liquid phase to form a protective film and reduce sliding friction.

The relative density distribution of atoms in SOP molecules at the direction of *z*-axis was given in Fig. 9. After a period of time, the adsorption peak of lubricant molecules on the ferric oxide and silicon oxide surface appeared at 6.8 and 12.0 Å, respectively. The concentration of lubricant molecules increases on the surface of iron oxide and silica and decreases in the middle, indicating that SOP molecules have good physical adsorption ability on the surface of iron oxide and silica.

The interaction of ferric oxide or silicon oxide matrix and SOP molecules were calculated based on the Eq. (3) in Fig. 10.

$$E_{\text{inter}} = E_{\text{total}} - (E_{\text{m}} + E_{\text{SOP}}) \tag{3}$$

where E_{inter}, E_{m} and E_{SOP} represent the interaction energy, the surface energy of ferric oxide or silicon oxide and the surface energy of SOP molecules, respectively. The average adsorption energy

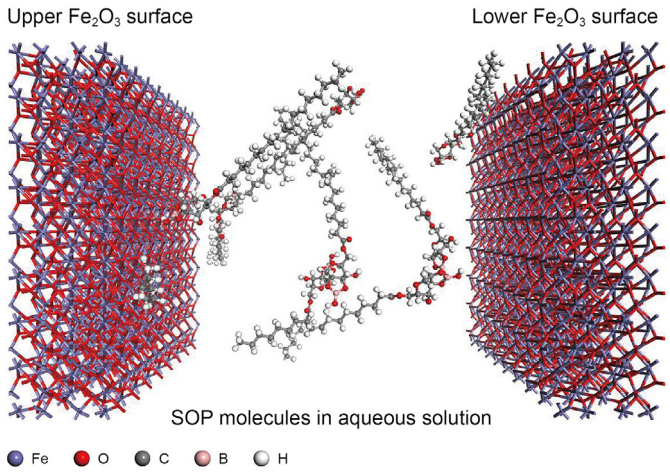

Fig. 8. Snapshot of SOP molecules adsorbed on the ferric oxide surface during simulations.

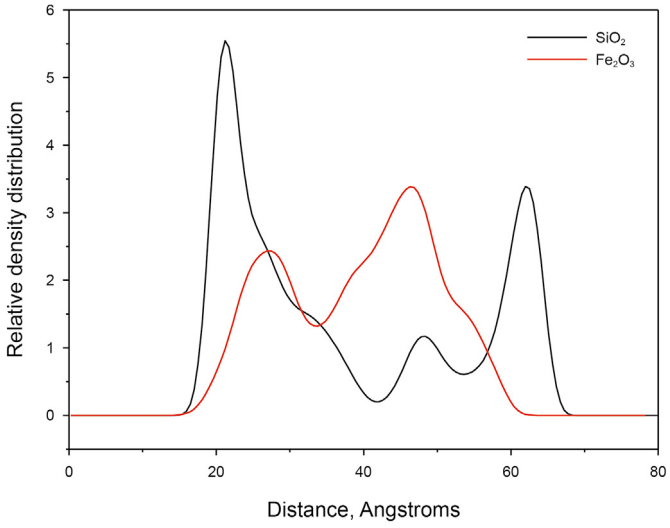

Fig. 9. The concentration profile of atoms in SOP molecules at the direction of *z*-axis.

between lubricant molecules and ferric oxide or silicon oxide was 24.49 and 75.63 kcal/mol, respectively. It is found that the vanderWaals force was the main interaction between SOP molecules and ferric oxide or silicon oxide, which is in consistency with previous studies. The ester and hydroxyl groups in SOP molecules could form hydrogen bonds with oxygen atoms on the surface of ferric oxide, which provided favorable conditions for the reaction of boron atoms under extreme pressure, and thus could explain the phenomenon that grafted compound exhibited better lubricating ability than mixed lubricants system. Due to the limitations of MD simulations, the reaction between boron and ferric oxide cannot be observed, and thus XPS analysis were carried out.

3.5. XPS analysis

To explore further, the lubrication mechanism and elemental distribution of friction films on wear surfaces in aqueous lubrication systems were analyzed from the XPS peak splitting fitted spectra in Fig. 11. The fitted peaks of C1s consisted of two parts located at 284.78 eV (C═C), 288.52 eV (C═O), indicating that SOP adsorbs on the metal surface at the sliding interface, producing a physisorbed film. From the O1s spectrum, three representative peaks labeled at 529.98, 532.04, and 533.16 eV correspond to Fe–O, Fe–O–B, and C═O, respectively. All these peaks show the information that the tribochemical reaction occurs on the sliding parts. The combined analysis of the C1s and O1s peaks further indicates the formation of a tribochemical reaction film at the friction interface. The B1s signal clearly shows the presence of two characteristic peaks at 189.97 eV (Fe–O–B) and 191.56 eV (B–O), indicating that the tribochemical reactions contributed by the active element boron in the SOP molecule occur mainly at the interface, resulting in effective lubricity. A more favorable analysis can be obtained from the valence of the Fe2p signal, specifically delineated by peaks at 722.12, 711.68, 709.03, and 707.05 eV, respectively, which are attributed to possible compounds on the wear point surface, namely Fe–O–B, FeOOH, Fe–O, and Fe. All these analyses show that the lubricant SOP is still able to form physisorbed friction film on the friction surface under high temperature and high salt conditions, while the tribochemical reaction occurs during the sliding interaction to form a chemically reactive friction film. Their synergistic effect makes the direct friction between drilling tool and drilling tool, drilling tool and well wall change to friction between lubricating films under high temperature and high salt conditions, thus significantly reducing frictional resistance and wear.

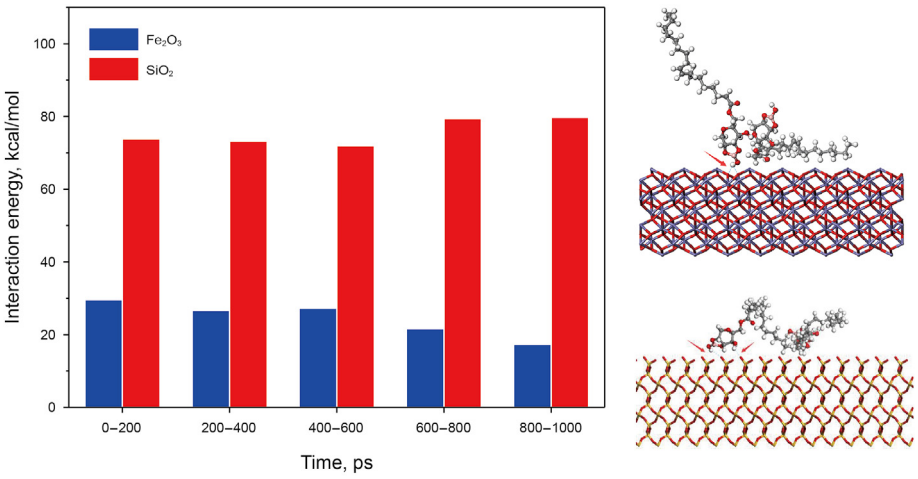

Fig. 10. The interaction energy evolution between the ferric oxide or silicon oxide layers and SOP molecules (left). Snapshot of the interaction between SOP molecules and the ferric oxide or silicon oxide layer via hydrogen bond (blue dashed line) (right).

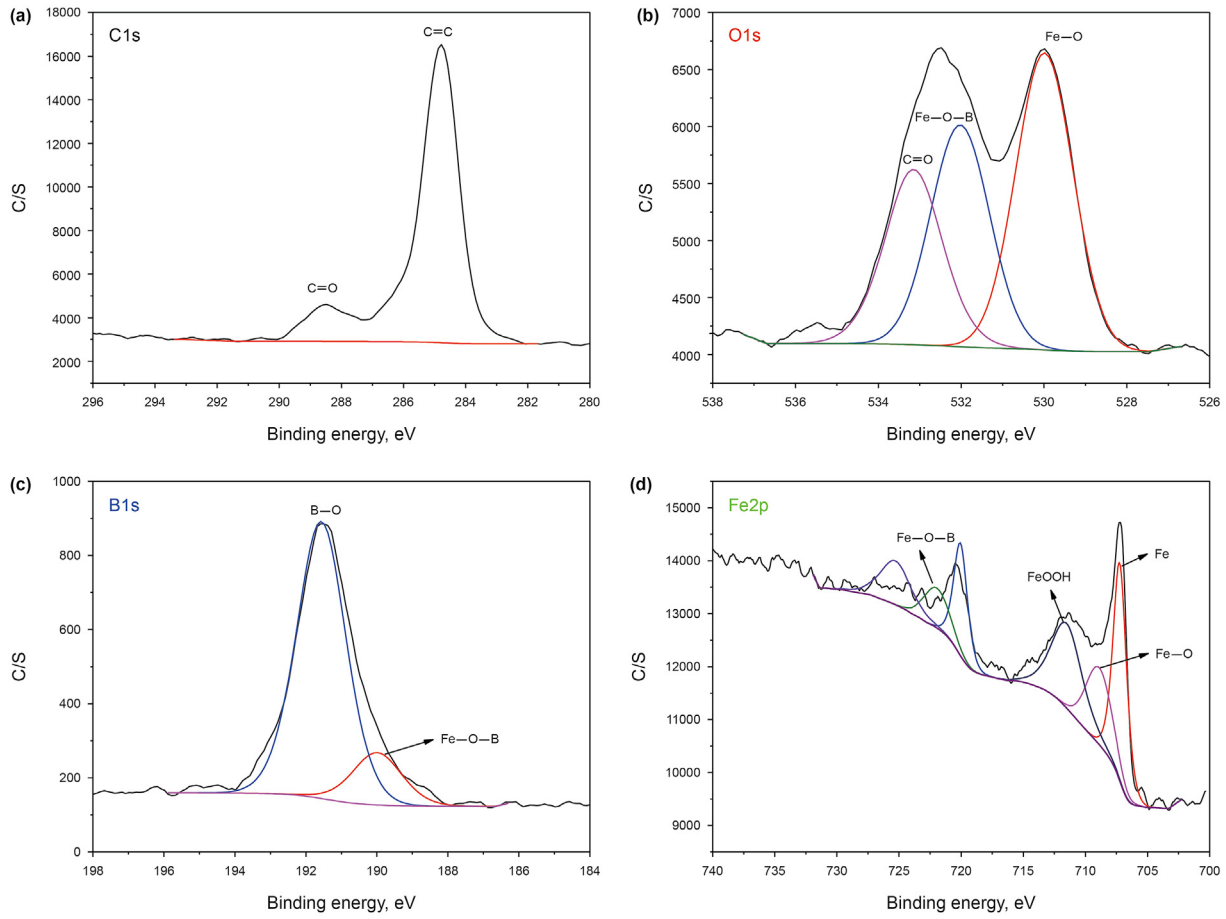

Fig. 11. XPS spectra of wear surfaces lubricated by lubricant SOP.

3.6. Mechanism analysis

Based on the analysis of the above experimental results, the lubrication mechanism of lubricant SOP is put forward. One end of SOP molecular structure is a polar group, which can be adsorbed on the drilling tool or well wall through van der Waals force and hydrogen bond. While the other end is a non-polar hydrophobic group, which is free in the drilling fluid to form a "brush" like "isolation layer", so that the friction between the drilling tool and the well wall becomes the friction between the "isolation layer", which effectively improves the lubricity. At the same time, the adsorption of SOP also provides favorable conditions for the reaction of boron atoms under extreme pressure. Under the conditions of high temperature and extreme pressure, boron atoms react with metal atoms on the surface of drilling tools to form a firm chemical reaction film and reduce the shear strength, which can effectively protect the metal surface from adhesive wear and reduce the friction coefficient. Under the synergistic action of the "isolation layer" formed by SOP molecules and extreme pressure reaction film, the drilling fluid added with SOP under high temperature and high salt conditions can still maintain good lubricity.

3.7. Environmental Aspects

As shown in Table 1, the EC_{50} value of SOP is 78620, which is greater than 30,000, which indicates that it is non-toxic. The BOD_5 is 294 mg/L and the COD is 1010 mg/L. It has a BOD_5/COD value of 29.1%, which is an easily degradable product and meets the emission standards. The toxicity and biodegradability tests indicate that SOP is an environmentally friendly lubricant.

4. Conclusions

In this study, an environmentally friendly anti-high temperature and high salt lubricant SOP was successfully prepared. Experimental results show that the reduction of lubrication coefficient of the base slurry with 1% SOP remained at 81.5% at 210 °C and 30% NaCl. After adding 1% SOP, the wear volume decreased by 94.11% compared with the base slurry. The lubricating performance of SOP is better than that of synthetic fatty acid ester GM and mineral oil based extreme pressure lubricant HEP-1. And it can still maintain good lubrication performance under high temperature and high salt conditions. Molecular dynamics simulation proves that SOP can form a physical adsorption film on the drilling tool or well wall under the action of van der Waals force and hydrogen bonding. At the same time, under extreme pressure conditions, SOP reacts with the metal atoms on the surface of the drilling tool to form a strong protective film, which can effectively protect the metal surface from adhesion wear and reduce the friction coefficient. In addition, SOP

Table 1
Environmental indicator evaluation results.

Indicator	Measured value	Standard value	Classification
EC_{50}, mg/L	78600	≥30000	Nontoxic
BOD_5:COD, %	29.1	>25	Easily degradable

is non-toxic and environmental friendly. SOP has a broad application prospect as an efficient and environmentally friendly lubricant for high-temperature and high-salt water-based drilling fluids.

Declaration of competing interest

We declare that we have no financial and personal relationships with other people or organizations that can inappropriately influence our work, there is no professional or other personal interest of any nature or kind in any product, service and/or company that could be construed as influencing the position presented in, or the review of, the manuscript entitled.

Acknowledgements

This work was financially supported by National Natural Science Foundation of China (No. 52074330), National Natural Science Foundation of China Major Projects (No. 51991361).

References

Aarrestad, T.V., 1994. Torque and drag-two factors in extended-reach drilling. J. Petrol. Technol. 46 (9), 800–803. https://doi.org/10.2118/27491-PA.

Bahlakeh, G., Ramezanzadeh, B., Ramezanzadeh, M., 2018. New detailed insights on the role of a novel praseodymium nanofilm on the polymer/steel interfacial adhesion bonds in dry and wet conditions: an integrated molecular dynamics simulation and experimental study. J. Taiwan Inst. Chem. Eng. 85, 221–236. https://doi.org/10.1016/j.jtice.2018.01.013.

Berro, H., Fillot, N., Vergne, P., 2010. Molecular dynamics simulation of surface energy and ZDDP effects on friction in nano-scale lubricated contacts. Tribol. Int. 43 (10), 1811–1822. https://doi.org/10.1016/j.triboint.2010.02.011.

Borugadda, V.B., Goud, V.V., 2016. Improved thermo-oxidative stability of structurally modified waste cooking oil methyl esters for bio-lubricant application. J. Clean. Prod. 112, 4515–4524. https://doi.org/10.1016/j.jclepro.2015.06.046.

Briscoe, B., Cann, P., Delfino, A., et al., 2001. Lubrication of water-based clay suspensions. Tribol. 39, 331–340. https://doi.org/10.1016/S0167-8922(01)80118-8.

Chang, X., Sun, J., Xu, Z., et al., 2019a. Synthesis of a novel environment-friendly filtration reducer and its application in water-based drilling fluids. Colloid Surf. A-Physicochem. Eng. Asp. 568, 284–293. https://doi.org/10.1016/j.colsurfa.2019.01.055.

Chang, X., Sun, J., Xu, Z., et al., 2019b. A novel nano-lignin-based amphoteric copolymer as fluid-loss reducer in water-based drilling fluids. Colloid Surf. A-Physicochem. Eng. Asp. 583, 123979. https://doi.org/10.1016/j.colsurfa.2019.123979.

Chhowalla, M., Amaratunga, G.A., 2000. Thin films of fullerene-like MoS 2 nanoparticles with ultra-low friction and wear. Nature 407 (6801), 164–167. https://doi.org/10.1038/35025020.

David, Ytrehus J., Taghipour, A., Golchin, A., et al., 2017. The effect of different drilling fluids on mechanical friction. J. Energy Resour. Technol. 139 (3). https://doi.org/10.1115/1.4035951.

Dong, R., Bao, L., Yu, Q., et al., 2020. Effect of electric potential and chain length on tribological performances of ionic liquids as additives for aqueous systems and molecular dynamics simulations. ACS Appl. Mater. Interfaces 12 (35), 39910–39919. https://doi.org/10.1021/acsami.0c11016.

Dong, X., Wang, L., Yang, X., et al., 2015. Effect of ester based lubricant SMJH-1 on the lubricity properties of water based drilling fluid. J. Pet. Sci. Eng. 135, 161–167. https://doi.org/10.1016/j.petrol.2015.09.004.

Humood, M., Ghamary, M.H., Lan, P., et al., 2019. Influence of additives on the friction and wear reduction of oil-based drilling fluid. Wear 422, 151–160. https://doi.org/10.1016/j.wear.2019.01.028.

Ji, G., Sun, T., Zhou, Q., et al., 2002. Constructed subsurface flow wetland for treating heavy oil-produced water of the Liaohe Oilfield in China. Ecol. Eng. 18 (4), 459–465. https://doi.org/10.1016/S0925-8574(01)00106-9.

Kania, D., Yunus, R., Omar, R., et al., 2015. A review of biolubricants in drilling fluids: recent research, performance, and applications. J. Pet. Sci. Eng. 135, 177–184. https://doi.org/10.1016/j.petrol.2015.09.021.

Lan, P., Iaccino, L.L., Bao, X., et al., 2020. The effect of lubricant additives on the tribological performance of oil and gas drilling applications up to 200. C. Tribol. Int. 141, 105896. https://doi.org/10.1016/j.triboint.2019.105896.

Li, W., Zhao, X., Li, Y., et al., 2015. Laboratory investigations on the effects of surfactants on rate of penetration in rotary diamond drilling. J. Pet. Sci. Eng. 134, 114–122. https://doi.org/10.1016/j.petrol.2015.07.027.

Liu, S., Chen, Z., Meng, Q., et al., 2017. Effect of graphene and graphene oxide addition on lubricating and friction properties of drilling fluids. Nanosci. Nanotechnol. Lett. 9 (4), 446–452. https://doi.org/10.1166/nnl.2017.2334.

Liu, X., Gao, L., Wang, Q., et al., 2021. Evaluation and application of poly (ethylene glycol) as lubricant in water-based drilling fluid for horizontal well in Sulige Gas Field. Polym. Int. 70 (1), 83–89. https://doi.org/10.1002/pi.6092.

Livescu, S., Craig, S., 2017. A critical review of the coiled tubing friction-reducing technologies in extended-reach wells. Part 1: lubricants. J. Pet. Sci. Eng. 157, 747–759. https://doi.org/10.1016/j.petrol.2017.07.072.

Ma, L., Luo, J., Zhang, C., et al., 2009. Film forming characteristics of oil-in-water emulsion with super-low oil concentration. Colloid Surf. A-Physicochem. Eng. Asp. 340 (1–3), 70–76. https://doi.org/10.1016/j.colsurfa.2009.03.006.

McGuiggan, P., Gee, M., Yoshizawa, H., et al., 2007. Friction studies of polymer lubricated surfaces. Macromolecules 40 (6), 2126–2133. https://doi.org/10.1021/ma061750h.

Nomura, A., Ohno, K., Fukuda, T., et al., 2012. Lubrication mechanism of concentrated polymer brushes in solvents: effect of solvent viscosity. Polym. Chem. 3 (1), 148–153. https://doi.org/10.1039/C1PY00215E.

Paswan, B.K., Mahto, V., 2020. Development of environment-friendly oil-in-water emulsion based drilling fluid for shale gas formation using sunflower oil. J. Pet. Sci. Eng. 191, 107129. https://doi.org/10.1016/j.petrol.2020.107129.

Philippon, D., De Barros-Bouchet, M.I., Lerasle, O., et al., 2011. Experimental simulation of tribochemical reactions between borates esters and steel surface. Tribol. Lett. 41, 73–82. https://doi.org/10.1007/s11249-010-9685-2.

Pi, Y., Zheng, Z., Bao, M., et al., 2015. Treatment of partially hydrolyzed polyacrylamide wastewater by combined Fenton oxidation and anaerobic biological processes. Chem. Eng. J. 273, 1–6. https://doi.org/10.1016/j.cej.2015.01.034.

Ramezanzadeh, M., Bahlakeh, G., Sanaei, Z., et al., 2019. Interfacial adhesion and corrosion protection properties improvement of a polyester-melamine coating by deposition of a novel green praseodymium oxide nanofilm: a comprehensive experimental and computational study. J. Ind. Eng. Chem. 74, 26–40. https://doi.org/10.1016/j.jiec.2019.01.037.

Rappe, A.K., Casewit, C.J., Colwell, K.S., et al., 1992. UFF, a full periodic table force field for molecular mechanics and molecular dynamics simulations. J. Am. Chem. Soc. 114 (25), 10024–10035. https://doi.org/10.1021/ja00051a040.

Razali, S., Yunus, R., Rashid, S.A., et al., 2018. Review of biodegradable synthetic-based drilling fluid: progression, performance and future prospect. Renew. Sustain. Energy Rev. 90, 171–186. https://doi.org/10.1016/j.rser.2018.03.014.

Saffari, H., Soltani, R., Alaei, M., et al., 2018. Tribological properties of water-based drilling fluids with borate nanoparticles as lubricant additives. J. Pet. Sci. Eng. 171, 253–259. https://doi.org/10.1016/j.petrol.2018.07.049.

Saidi, M., Pasc, A., El, Moujahid C., et al., 2020. Improved tribological properties, thermal and colloidal stability of poly-α-olefins based lubricants with hydrophobic MoS2 submicron additives. J. Colloid Interface Sci. 562, 91–101. https://doi.org/10.1016/j.jcis.2019.12.007.

Shah, F.U., Glavatskih, S., Antzutkin, O.N., 2013. Boron in tribology: from borates to ionic liquids. Tribol. Lett. 51 (3), 281–301. https://doi.org/10.1007/s11249-013-0181-3.

Shaji, S., Radhakrishnan, V., 2003. Analysis of process parameters in surface grinding with graphite as lubricant based on the Taguchi method. J. Mater. Process. Technol. 141 (1), 51–59. https://doi.org/10.1016/S0924-0136(02)01112-3.

Sönmez, A., Kök, M.V., Özel, R., 2013. Performance analysis of drilling fluid liquid lubricants. J. Pet. Sci. Eng. 108, 64–73. https://doi.org/10.1016/j.petrol.2013.06.002.

Sun, J.-S., Wang, Z.-L., Liu, J.-P., et al., 2022. Notoginsenoside as an environmentally friendly shale inhibitor in water-based drilling fluid. Petrol. Sci. 19 (2), 608–618. https://doi.org/10.1016/j.petsci.2021.11.017.

Sun, J., Chang, X., Lv, K., et al., 2020. Salt-responsive zwitterionic copolymer as tackifier in brine drilling fluids. J. Mol. Liq. 319, 114345. https://doi.org/10.1016/j.molliq.2020.114345.

Tadros, T., 2011. Interaction forces between adsorbed polymer layers. Adv. Colloid Interface Sci. 165 (2), 102–107. https://doi.org/10.1016/j.cis.2011.02.002.

Teer, D., 2001. New solid lubricant coatings. Wear 251 (1–12), 1068–1074. https://doi.org/10.1016/S0043-1648(01)00764-5.

Xiao, H., Liu, S., Chen, Y., et al., 2017. Impacts of polypropylene glycol (PPG) additive and pH on tribological properties of water-based drilling mud for steel-steel contact. Tribol. Lett. 110, 318–325. https://doi.org/10.1016/j.triboint.2017.02.025.

Xiao, H., Liu, S., Guo, Y., et al., 2016. Effects of microscale particles as antiwear additives in water-based slurries with abrasives. Tribol. Trans. 59 (2), 323–329. https://doi.org/10.1080/10402004.2015.1077410.

Zheng, Z., Shen, G., Wan, Y., et al., 1998. Synthesis, hydrolytic stability and tribological properties of novel borate esters containing nitrogen as lubricant additives. Wear 222 (2), 135–144. https://doi.org/10.1016/S0043-1648(98)00323-8.

Zhou, F.S., Xiong, Z.Q., Cui, B.L., et al., 2013. Effect of nitric acid on the low fluorescing performance of drilling fluid lubricant based animal and vegetable oils. J. Spectrosc. 2013. https://doi.org/10.1155/2013/269280.